[16] J. Crowell and R. H. Ritchie, Phys. Rev. **172**, 436 [1968].
[17] F. Fujimoto and K. Komaki, J. Phys. Soc. Japan **25**, 1679 [1968].
[18] Th. Kokkinakis and K. Alexopoulos, Phys. Rev. Lett. **28**, 1632 [1972].
[19] H. Ehrenreich and H. R. Philipp, Phys. Rev. **128**, 1622 [1962].
[20] Th. Kokkinakis, unpublished.
[21] R. H. Doremus, J. Chem. Phys. **40**, 2389 [1964].
[22] Free electron theory.
[23] J. L. Robins, Proc. Phys. Soc. **78**, 1177 [1961].

# An Absolute Atomic Scattering Factor for Germanium Obtained by Anomalous Transmission in a Bicrystal

J. F. C. Baker, M. Hart, and J. Helliar

H. H. Wills Physics Laboratory, Royal Fort, University of Bristol

(Z. Naturforsch. **28 a**, 553–557 [1973]; received 22 January 1973)

*Dedicated to Professor G. Borrmann on his 65th birthday*

Using the newly developed method of dynamical interference between anomalously transmitted waves in a crystal containing a non-diffracting zone [1], we have measured the real part of the atomic scattering factor for germanium at the value of $\sin\theta/\lambda$ corresponding to the 220 Bragg reflection. The result, $f_0 = 23.79 \pm 0.08$ electron units is in excellent agreement with values obtained in perfect crystal intensity measurements [2, 3] and from triple crystal rocking curve studies [4, 5] but significantly differs from the value obtained using Pendellösung fringes [3]. Finally, we seek to assess the reliability of each method by comparison with the corresponding results for silicon, concluding that the error probably lies in the Pendellösung result.

## Introduction

Provided that adequately homogeneous crystals, free from dislocations and planar defects, can be obtained there are several dynamical diffraction effects which may be used to obtain accurate values of structure factors without the need for accurate *absolute* intensity measurements.

Structure factors for germanium had already been obtained from absolute integrated intensity measurements by DeMarco and Weiss [2] when, in 1968, Batterman and Patel [3] made structure factor measurements on germanium using both the Bragg case integrated intensity and the Pendellösung methods. They found significant differences between the results obtained by the two methods. Similar differences seemed to be evident in the silicon data then available though, as we will see later, the Pendellösung results for silicon have since been revised. From measurements of the intrinsic diffraction profiles of germanium using a triple-crystal diffractometer Nakayama, Kikuta and Kohra [4] (1971) and Persson, Zielinska and Gerward [5] made quite independent structure factor measurements which seem to favour the previous integrated intensity results rather than Batterman and Patel's Pendellösung values. In an attempt to provide more independent evidence, we have used the method devised by Hart and Milne [1] to measure the absolute structure factor for the 220 Bragg reflection from germanium.

Reprint requests to Dr. M. Hart, H. H. Wills Physics Laboratory, Royal Fort, University of Bristol, *Bristol BS8 1TL*, England.

This interference effect, produced by a non-diffracting zone in a crystal, is in principle quite different from the Pendellösung effect because only one branch of the dispersion surface is involved. The method is described in detail in the original paper [1] where it was applied to silicon, yielding scattering factors within 0.1% of those obtained using Pendellösung fringes. Let us briefly recall the relevant theory and the approximations involved.

## Theoretical Background

We record the interference pattern obtained when a narrow divergent incident ribbon beam is Bragg reflected by a thick, perfect crystal which contains a narrow gap (Figure 1). Within the Borrmann fan various pairs of ray-paths, such as those illustrated, are possible between the point of incidence and the exit points. For a gap of zero thickness the pair of rays coalesce into one and these interference fringes disappear. In reciprocal space the two ray bundles are described by tie points A and B giving rise to energy flows inside the crystal inclined at angles $\alpha$ and $\beta$ respectively to the Bragg planes.

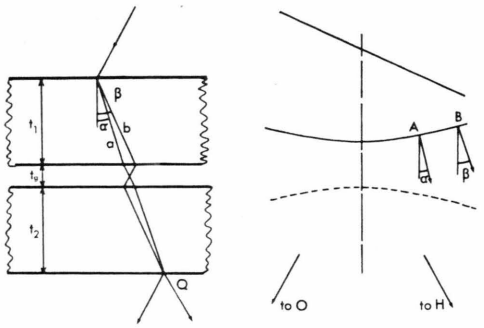


Fig. 1. Schematic diagram of the ray paths and tiepoints which are important in anomalous transmission through a crystal containing a gap.

For transmission in the symmetric case two such waves which intersect the exit surface at Q, having travelled along path a and b, have amplitudes [6]

$$\left.\begin{aligned} D_a &= D(t_1+t_2)^{-\frac{1}{2}} f_1(\Delta\Theta)\exp\{-i(\Phi_0-\pi/2)\},\\ D_b &= D(t_1+t_2)^{-\frac{1}{2}} f_2(\Delta\Theta)\exp\{-i(\Phi_h-\pi/2)\}.\end{aligned}\right\} \quad (1)$$

$D$ is a constant and $f_1(\Delta\Theta)$, $f_2(\Delta\Theta)$ describe the variation of amplitude with angle of incidence. The phases $\Phi_0$ and $\Phi_h$ are given by

$$\left.\begin{aligned} \Phi_0 &= \frac{\pi}{\Delta_0}(t_1+t_2)(1-P_\alpha{}^2)^{\frac{1}{2}},\\ \Phi_h &= \frac{\pi}{\Delta_0}(t_1+t_2)(1-P_\beta{}^2)^{\frac{1}{2}}\end{aligned}\right\} \quad (2)$$

where

$$\Delta_0 = \lambda\cos\Theta/C(\chi_h\chi_{\bar{h}})^{\frac{1}{2}} \quad (3)$$

and the deviation parameters $P_\alpha$, $P_\beta$ are defined by

$$P_\alpha = \tan\alpha/\tan\Theta\,, \qquad P_\beta = \tan\beta/\tan\Theta\,. \quad (4)$$

$\chi_h$ and $\chi_{\bar{h}}$ are the $hkl$ and $\bar{h}\bar{k}\bar{l}$ coefficients in the Fourier expansion of the dielectric susceptibility $\chi$.

$$\chi_h = \frac{-e^2\lambda^2}{\pi m c^2 V}F_h \quad (5)$$

$\lambda$ is the X-ray wavelength, $\Theta$ the Bragg angle and $C$ is a factor which is 1 for the $\sigma$-case of polarisation and $|\cos 2\Theta|$ for the $\pi$-case. $e$, $m$ and $c$ are the usual fundamental constants. $F_h$ is the structure factor for the unit cell whose volume is $V$.

If the thickness $t_g$ of the non-diffracting zone is very much less than $t$ $(t=t_1+t_2)$, the combined thickness of the two crystal parts then, with errors estimated to be of the order of 0.2%, the intensity in the diffraction pattern is [1]

$$\begin{aligned} I_h \propto{}& \exp\{-\mu^\sigma t\}\cos^2\left[\frac{\pi}{\Delta_0{}^\sigma}t_g\overline{P}(1-\overline{P}^2)^{-\frac{1}{2}}\right]\\ &+|\cos 2\Theta|\exp\{-\mu^\pi t\}\cos^2\\ &\left[\frac{\pi}{\Delta_0{}^\sigma}|\cos 2\Theta|\,t_g\overline{P}(1-\overline{P^2})^{-\frac{1}{2}}\right] \end{aligned} \quad (6)$$

where

$$\mu^\sigma = \mu\frac{\cos\Delta}{\cos\Theta}\left[1-\frac{\chi_{ih}}{\chi_{i0}}(1-\overline{P}^2)^{\frac{1}{2}}\right],$$

$$\mu^\pi = \mu\frac{\cos\Delta}{\cos\Theta}\left[1-|\cos 2\Theta|\,\frac{\chi_{ih}}{\chi_{i0}}(1-\overline{P}^2)^{\frac{1}{2}}\right].$$

Here, $\overline{P}=\frac{1}{2}(P_\alpha+P_\beta)=\tan\Delta/\tan\Theta$ and $\mu$ is the normal photoelectric absorption coefficient. $\chi_{i0}$, $\chi_{ih}$ are the imaginary parts of $\chi_0$ and $\chi_h$ respectively; their ratio has been measured by Okkerse [7] who obtained the value 0.9592 using copper K$\alpha$ radiation. The reliability of this phenomenological treatment of the absorption [Eq. (6)] was confirmed in silicon by the good agreement obtained by Hart and Milne [1] between the calculated profile $I_h$ and the densitometer traces of experimental interference patterns.

If we expand the argument of the first cosine term in Eq. (6) to first order in $\overline{P}$ we find that the fringe spacing $\Delta$ is given by

$$\Delta = \Delta_0(t_1+t_2)\tan\Theta/t_g\,. \quad (7)$$

Identical fringes have been obtained by Bonse and te Kaat [8] in the optically equivalent case of a slightly defocused X-ray interferometer. Their Eq. (42) is identical to (7) if $(t_1+t_2)$ is equal to the total thickness of the X-ray interferometer wafers and $t_g$ is the defocus distance.

Using Eq. (7) we can make rough estimates of some of the experimental parameters. For $t=4$ mm, $t_g=0.3$ mm, and $F_h=186$ we calculate $\Delta\cong 40\,\mu$m for the 220 reflection. It is interesting to note that, at least for the dominant $\sigma$-polarisation state, the fringe spacing is independent of the X-ray wavelength (apart from the effects of anomalous dispersion) for a particular Bragg reflection.

## Experimental Arrangement

The germanium crystal was grown in the [111] direction and was n-type with a resistivity of greater than 40 Ohm cm. After checking by the Lang method that the material was dislocation free, double crystal topographs were obtained in the Bragg case using the $\bar{4}40$-Bragg reflection of copper K$\alpha$ radiation from a $(\bar{2}11)$ surface cut on the boule. No trace of growth bands was found, indicating that the homogeneity of this germanium was adequate for these interference experiments.

A stepped sample was cut using conventional diamond coated slitting saws so that in one exposure

several different crystal thicknesses could be investigated. After cutting, the damaged surface was removed by chemical polishing.

The specimen was mounted on a calibrated slide unit so that diffraction patterns could be obtained at known positions with respect to a reference edge in the sample. Interference patterns were recorded on nuclear emulsion plates type L4-100 $\mu$m placed normal to the diffracted beam. After the exposures had been made the crystal was cut parallel to the Bragg planes through the line of incidence so that the crystal thicknesses $t_1$ and $t_2$ and the gap width $t_g$ could be measured with a travelling microscope. A typical microdensitometer trace, of step 3 on plate B, is shown in Figure 2. With silver $K\alpha_1$ radiation exposure times of 60 hrs were required when the collimator slit was 22 $\mu$m wide. All the experimental results are collected together in Table 1.

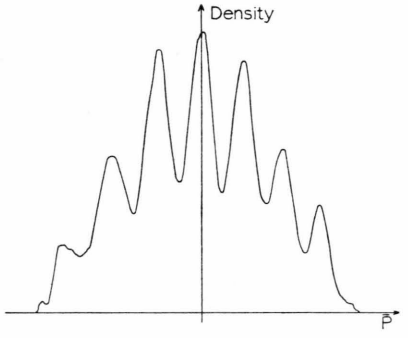


Fig. 2. Experimental microdensitometer record of the intensity distribution measured along a line normal to the diffracted beam. Plate B step 3.

Table 1. Experimental results and derived structure factors (all lengths are measured in $\mu$m).

| Plate A | $t_1$ | $t_g$ | $t_2$ | $l_1$ | $l_2$ | $F_h$ |
|---|---|---|---|---|---|---|
| step 1 | 1974 | 298 | 2019 | 71.0 | 143 | 187.0 |
| 2 | 2137 | 288 | 2038 | 80.0 | 155 | 183.7 |
| 3 | 2320 | 286 | 2046 | 82.0 | 159 | 188.8 |
| 4 | 2540 | 285 | 2053 | 87.0 | 172 | 185.0 |
| **Plate B** | | | | | | |
| step 1 | 1974 | 296 | 2019 | 72.0 | 147 | 184.0 |
| 2 | 2136 | 287 | 2035 | 78.5 | 156 | 184.9 |
| 3 | 2313 | 284 | 2050 | 82.0 | 161 | 188.4 |
| 4 | 2548 | 285 | 2058 | 88.0 | 167 | 188.9 |
| **Plate C** | | | | | | |
| step 1 | 1964 | 302 | 2013 | 73.0 | 141 | 184.1 |
| 2 | 2137 | 293 | 2036 | 77.0 | 152 | 185.5 |
| 3 | 2308 | 291 | 2039 | 82.0 | 158 | 185.8 |
| 4 | 2540 | 290 | 2048 | 83.0 | 165 | 191.7 |

The patterns computed from Eq. (6) were very similar to the patterns obtained before[1] in silicon, showing fringes with almost 100% contrast. Since the collimator slit was comparable in width to the spacing of fringes we recomputed the pattern using a slit smearing function which averaged the value of $I_h$ over a region 22 $\mu$m wide and also calculated the optical density mean over a 20 $\mu$m slit width, corresponding to the transmission function of our optical densitometer. This second operation had little additional effect on the intensity profile. The dominant X-ray collimator slit smearing operation altered the intrinsic fringe spacing in $I_h$ by about 2% and roughly halved the fringe contrast. A typical computed intensity profile is illustrated in Fig. 3 for step 3 of plate B with $F_h = 186$.

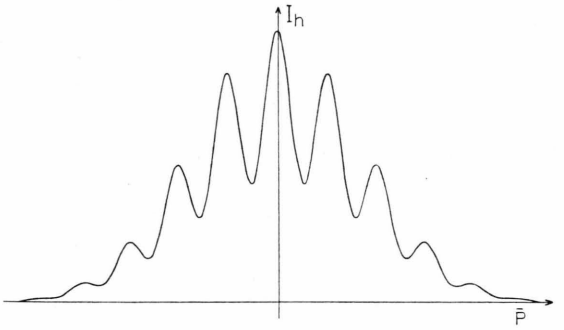


Fig. 3. Theoretical intensity distribution $I_h$ for the diffracted beam measured along the exit surface of the crystal. The chosen parameters are appropriate to plate B, step 3 with $F_h = 186$.

For each experimental result we computed a profile like the one illustrated, using two different values for the structure factor. Since the main influence of changes in $F_h$ is to change the scale of the abscissa, without changing the fringe profiles, we were able to interpolate from these intensity profiles to obtain the value of $F_h$ which best fitted the five central fringes of the experimental pattern. This value is listed in the final column of Table 1. $l_1$ and $l_2$ are the separations of the first and second order fringes respectively on the nuclear emulsion plates.

The mean value of $F_h$ is 186.6 with a standard error of $\pm 0.7$.

In these experiments the anomalous absorption effect is very strongly manifested as the following numbers show. For the thinnest sample used, $t = 3977$ $\mu$m, the normal absorption coefficient is $\exp\{-67.5\}$ or $4.8 \times 10^{-30}$ using the value[3] $\mu = 168\ \mathrm{cm}^{-1}$. On the other hand, at the centre of the reflecting range $\exp\{-\mu^{\sigma} t\}$ is 0.0637 while $\exp\{-\mu^{\pi} t\}$ is 0.0051. Only 8% of the intensity is

due to $\pi$-polarised radiation and this is one reason why Eq. (6) is so successful in describing the observed intensity profiles. The attenuation coefficients for waves on the other branch of the dispersion surface range from $4.8\times10^{-30}$ far off the Bragg angle to $3.7\times10^{-58}$ at the middle of the range of reflection for $\sigma$-polarised radiation. Therefore, strongly absorbed wavefields have no influence whatever in these patterns. Even at the second order fringes where $\bar{P}\cong\pm0.11$ the polarisation ratio is still about 8%.

## Comparison with Previous Results

We will reduce our structure factors to zero wavelength using [9] $\Delta f'=+0.36$ and adopt [10] $\Theta_M=290$ °K, so that [11] $B=0.567$ Å$^2$ at 20 °C. Then we have

$$f_0=23.79\pm0.08 \text{ for } \sin\Theta/\lambda=0.250 \text{ Å}^{-1}.$$

In Table 2 we have collected together all of the relevant previous single crystal scattering factor measurements. Where necessary we have modified the values slightly by using Cromer's [9] dispersion corrections rather than those used by the original authors.

Table 2. Measured values of $f_0$ for germanium at $\sin\theta/\lambda=0.250$ Å$^{-1}$.

| Method | $f_0$ | Radiation | $\Delta f'$ |
|---|---|---|---|
| Intensity [2] | $23.89\pm0.2$ | MoK$\alpha_1$ | +0.21 |
| Intensity [3] | $23.94\pm0.2$ | AgK$\alpha$ | +0.36 |
| Pendellösung [3] | $24.44\pm0.25$ | AgK$\alpha$ | +0.36 |
| Pendellösung [5] | $23.81\pm0.35$ | MoK$\alpha_1$ | +0.21 |
| Profile [4] | $23.78\pm0.017$ | CuK$\alpha_1$ | −1.31 |
| Gap crystal | $23.79\pm0.08$ | AgK$\alpha_1$ | +0.36 |

All but the Pendellösung result [3] are in excellent agreement. In an attempt to establish the pedigree of each method we will briefly examine the corresponding results for silicon where much more information is available. Let us concentrate in Table 3 on those reflections to which most of the independent methods have been applied.

All of the silicon results agree to within experimental errors or 0.2% whichever is larger so that we must regard all of these perfect crystal methods as reliable absolute methods. It follows then that Batterman and Patel's [3] Pendellösung measurement probably contains an error which is not intrinsic to the Pendellösung method. Perhaps it is important to remember that they did their measurements using integrated intensities, whereas all the Pendellösung measurements recorded in Table 3 were made on section patterns [14]. In the final part we examine in some detail, but without a forceful conclusion, possible systematic errors in Batterman and Patel's application of Pendellösung fringes to the measurement of structure factors.

## Integrated Intensity Pendellösung Measurements

For simplicity of discussion let us consider only one polarisation component. In the approximation of zero absorption, the integrated intensity obtained by the plane wave theory is exactly the same as the integrated intensity obtained using the spherical wave theory [15]. Batterman and Patel made the reasonable assumption that this is also true if absorption is present. Kato [16] has since shown that the two theories give different results viz.;
for plane waves

$$R_h(y)=\tfrac{1}{2}\pi\exp\{-\mu t\sec\Theta\}\cdot\Big\{\underbrace{\int_0^{2A}J_0(\varrho)\,\mathrm{d}\varrho}_{W}+\underbrace{\sum_{n=1}^{\infty}(1/n!\,n!)\,(h/2)^{2n}}_{V}\Big\} \tag{8}$$

whereas, from the spherical wave theory

$$R_h(y)=\tfrac{1}{2}\pi\exp\{-\mu t\sec\Theta\}[(1+K^2)/(1-g^2)]^{\frac{1}{2}}\Big\{\underbrace{\int_0^{2A(1-g^2)^{1/2}}J_0(\varrho)\,\mathrm{d}\varrho}_{W^*}+\underbrace{\sum_{n=1}^{\infty}(1/n!\,n!)\,(h/2)^{2n}\,g_{2n+1}\,[2A(1-g^2)^{\frac{1}{2}}]}_{V^*}\Big\} \tag{9}$$

| Method | $f_0(111)$ | $f_0(220)$ | $f_0(422)$ | $f_0(333)$ |
|---|---|---|---|---|
| Intensity [2] | 10.80 ±.08 | 8.70 ±.06 | 6.82 ±.1 | 6.49 ±.08 |
| Pendellösung [12] | 10.738±.002 | 8.678±.002 | — | 6.445±.003 |
| Pendellösung [13] | 10.739±.006 | 8.651±.009 | 6.711±.009 | 6.429±.006 |
| Profile [4] | 10.779±.008 | — | 6.708±.006 | 6.442±.013 |
| Gap crystal [1] | — | 8.658±.017 | — | — |

Table 3. Atomic scattering factors for silicon.

where $A$ is proportional to the crystal thickness, $K=(\chi_{hi}\chi_{\bar{h}i})^{\frac{1}{2}}/(\chi_{hr}\chi_{\bar{h}r})^{\frac{1}{2}}$ and $g=0$ ini the symmetric Laue case. Now Batterman and Patel worked in the symmetric Laue case so that the Waller integrals $W$ and $W^*$ are equal. In effect, this means that Batterman and Patel's assumption can be justified. The second terms $V$ and $V^*$ describe the background on which the Pendellösung fringes are measured. Using the values of the $g_{2n+1}$ functions tabulated by Kato [15] we found no significant differences between the Pendellösung fringe spacings calculated from these two equations.

The spherical wave theory leads to Eq. (9) for the integrated reflection after an *incoherent* spatial integration over the exit surface of the crystal. In Batterman and Patel's investigation, the reciprocity theorem is invoked to show that the intensity at a point on the exit surface involves the same integration over the entrance surface. In their practical situation it seems to us that the illumination is *partially coherent* and, though we are unable to make an estimate of the influence of the degree of coherence on the integrated intensity, we suppose that fringe shifts of one tenth of a fringe spacing (which is more than enough to bring the results into agreement) might occur.


[1] M. Hart and A. D. Milne, Acta Cryst. A **26**, 223 [1970].
[2] J. J. DeMarco and R. J. Weiss, Phys. Rev. **137**, A 1869 [1965].
[3] B. W. Batterman and J. R. Patel, J. Appl. Phys. **39**, 1882 [1968].
[4] K. Nakayamu, S. Kikuta, and K. Kohra, Phys. Pett. **37** A, 29 [1971].
[5] E. Persson, E. Zielińska-Rohozińska, and L. Gerward, Acta Cryst. A **26**, 514 [1970].
[6] A. Authier, A. D. Milne, and M. Sauvage, Phys. Stat. Sol. **26**, 469 [1968].
[7] B. Okkerse, Philips Res. Rept. **17**, 464 [1962].
[8] U. Bonse and te Kaat, Z. Phys. **243**, 14 [1971].
[9] D. T. Cromer, Acta Cryst. **18**, 17 [1965].
[10] B. W. Batterman and D. R. Chipman, Phys. Rev. **127**, 690 [1962].
[11] B. Dawson, Proc. Roy. Soc. **298** A, 395 [1967].
[12] S. Tanemura and N. Kato, Acta Cryst. A **28**, 69 [1972].
[13] P. J. E. Aldred and M. Hart, Proc. Roy. Soc. **A 332**, 223 [1973].
[14] A. R. Lang, Acta Metall **5**, 358 [1957].
[15] N. Kato, Acta Cryst. **14**, 627 [1961].
[16] N. Kato, J. Appl. Phys. **39**, 2231 [1968].